

Correlated fluctuations in the $^{89}\text{Y}(^{19}\text{F},x)\gamma$ excitation functions

T. Suomijärvi, B. Berthier, R. Lucas, and M. C. Mermaz

Service de Physique Nucléaire—Métrologie Fondamentale, Centre d'Etudes Nucléaires de Saclay, 91191 Gif sur Yvette Cedex, France

J. P. Coffin, G. Guillaume, B. Heusch, F. Jundt, and F. Rami

Centre de Recherches Nucléaires and Université Louis Pasteur, 67037 Strasbourg Cedex, France

(Received 3 June 1986; revised manuscript received 16 March 1987)

Excitation functions have been measured for different fragments produced in the $^{89}\text{Y}(^{19}\text{F},x)\gamma$ reactions between 135 and 143.25 MeV incident energy in 250 keV steps. Cross section fluctuations correlated in atomic number and detection angle are observed with a coherence width of 200–500 keV. Lifetimes have been deduced and are of the order of a complete nuclear rotation. The data can be explained in terms of quasimolecular configurations and/or an orbiting situation in a dinuclear system.

I. INTRODUCTION

Long lifetime reactions, for which, however, all the degrees of freedom of the system have not reached a statistical equilibrium, have been recently observed in light nuclear collisions.^{1–3} Such reactions may be described in terms of orbiting which may correspond to quasimolecular state formation.

An elegant way to study the validity of this hypothesis is to rely on the recent approach of Brink and Dietrich⁴ based on the study of Ericson fluctuations in dissipative collisions. These authors have generalized the Ericson's calculation of the energy autocorrelation function for deeply inelastic collisions. Their developments are probably applicable only to light systems for which the number of unresolved final channels is reasonably small and, hence, the autocorrelation functions measurable. A study of the autocorrelation function permits a determination of the average coherence width Γ and thus of the corresponding average lifetime $\tau = \hbar/\Gamma$.

We have recently observed such a long lifetime process, departing from the compound nucleus formation, in the $^{19}\text{F} + ^{89}\text{Y}$ reaction performed at 140 MeV incident energy.^{1,2} The outgoing fragments ($5 \leq Z \leq 11$) have fully relaxed kinetic energies. They present isotropic angular distributions in the backward hemisphere and their corresponding lifetimes, deduced from a Regge pole analysis^{5,6} and a Strutinsky parametrization,⁷ are found to be of about 10^{-21} s.

In order to obtain a more accurate determination of these τ values and to examine in more detail the possible existence of quasimolecular configurations, we have investigated the $^{19}\text{F} + ^{89}\text{Y}$ reaction by measuring the yield excitation functions of various outgoing fragments between 135.00 and 143.25 MeV in 250 keV steps. Strong fluctuations of the yields have been observed and analyzed in the framework of two statistical approaches based, on one hand, on Z and angle cross-correlation methods, and, on the other, on autocorrelation function analysis.

II. EXPERIMENTAL METHOD

The ^{19}F beam was delivered by the 18 MV Strasbourg Tandem accelerator. Self-supporting ^{89}Y targets of $100 \mu\text{g}/\text{cm}^2$ were used. Such a thickness induces an energy loss of 230 keV for the incident ^{19}F ions, which is less than the energy increment used in the present experiment. The outgoing fragments were detected with three telescope counters. Each of them consisted of a 10 cm long ionization chamber, filled with isobutane, to generate a ΔE signal and a solid state detector to produce an E signal. These counters were located at $\theta_{\text{lab}} = 60^\circ$, 120° , and 160° , where only fragments yielded by strongly relaxed processes are detected, as demonstrated by the work of Ref. 2. (See Fig. 3 of Ref. 2.) The data collected in the various runs were normalized by reference to the Rutherford elastic scattering counting rates measured, at 12.5° and -12.5° with respect to the beam axis, with monitoring solid state counters.

III. EXPERIMENTAL RESULTS

Some examples of energy spectra corresponding to several outgoing fragments identified by their Z are presented in Fig. 1. They were measured at $\theta_{\text{lab}} = 60^\circ$ for an incident energy of 140.25 MeV. These spectra with fair statistics indeed exhibit a strong damping in energy. The excitation functions of various fragments, measured at $\theta_{\text{lab}} = 60^\circ$, 120° , and 160° , are presented in Figs. 2–4, respectively. The error bars are purely statistical and are clearly less than the size of the amplitudes of the observed fluctuations. The straight solid lines represent the averaged cross sections used in the statistical fluctuation analysis. They were deduced from a least squares fit applied to the experimental data. The cross sections shown in Fig. 5 correspond to the addition of the partial $Z = 8$, 10, and 11 cross sections. The fact that strong fluctuations subsist at the three angles after having added several excitation functions means that the fluctuations observed

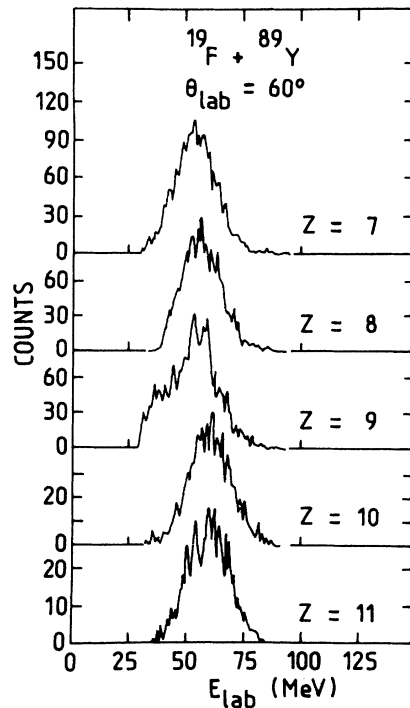


FIG. 1. Energy spectra of various ejectiles identified by their charge Z .

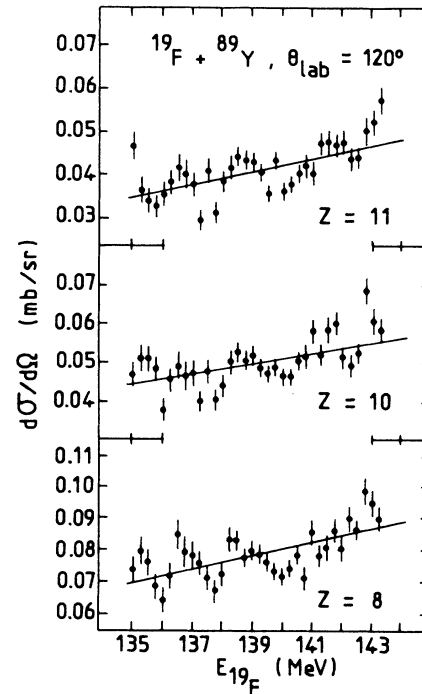


FIG. 3. Excitation functions, of three ejectiles, measured at 120° for the $^{89}\text{Y}(^{19}\text{F},x)y$ reaction. The straight solid lines represent the average cross section used in the statistical analysis.

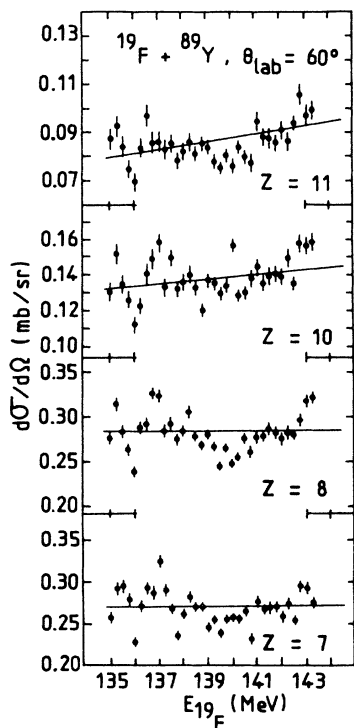


FIG. 2. Excitation functions, of various ejectiles identified by their atomic number, measured at 60° for the $^{89}\text{Y}(^{19}\text{F},x)y$ reaction. The straight solid lines represent the average cross sections used in the statistical analysis.

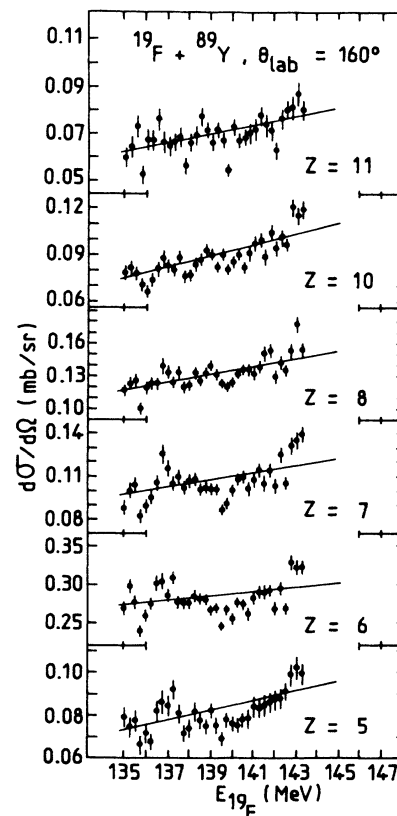


FIG. 4. Excitation functions, of various ejectiles, measured at 160° for the $^{89}\text{Y}(^{19}\text{F},x)y$ reaction. The straight solid lines represent the average cross section used in the statistical analysis.

in the cross sections of each individual Z are tiedly correlated. These summed excitation functions allow study of the cross-section fluctuations with better statistics.

IV. STATISTICAL ANALYSIS

The data obtained in the present work have been studied in the framework of a statistical analysis.^{8,9} In order to compare the fluctuations observed here to those in-

duced by the statistical deexcitation of a compound nucleus, we have, first, analyzed our data in terms of Z and θ cross correlations.

A. Cross-correlation analysis

At a particular θ angle, the Z cross-correlation coefficients have been calculated by using the following relationship:³

$$C(Z_1, Z_2) = [C(Z_1)C(Z_2)]^{-1/2} \frac{\langle [\sigma(E, Z_1) - \langle \sigma(Z_1) \rangle][\sigma(E, Z_2) - \langle \sigma(Z_2) \rangle] \rangle}{\langle \sigma(Z_1) \rangle \langle \sigma(Z_2) \rangle} \quad (1)$$

The θ cross-correlation coefficients $C(\theta_1, \theta_2)$, for a fragment of a given Z , are similar to (1), with the exception that Z_1 and Z_2 are replaced by θ_1 and θ_2 , respectively. In these relationships the angular brackets stand for the arithmetical average. The $C(Z_1, Z_2)$ and $C(\theta_1, \theta_2)$ coefficients obtained are reported in Tables I and II, respectively. The error bars were calculated by using the formula in Table 3 of Ref. 9. The Z cross-correlation coefficients are large compared to those corresponding to a pure statistical deexcitation, since in this latter case they

should be theoretically equal to zero when Z_1 is different from Z_2 . Similarly, except for two cases, all the θ cross-correlation coefficients, given in Table II, exceed 0.5. These values are in conflict with those expected from the compound nucleus decay, which implies a small angular coherence width, equal to $1/l_g$, where l_g is the arithmetical average between the grazing partial waves in the entrance and the exit channels.¹⁰

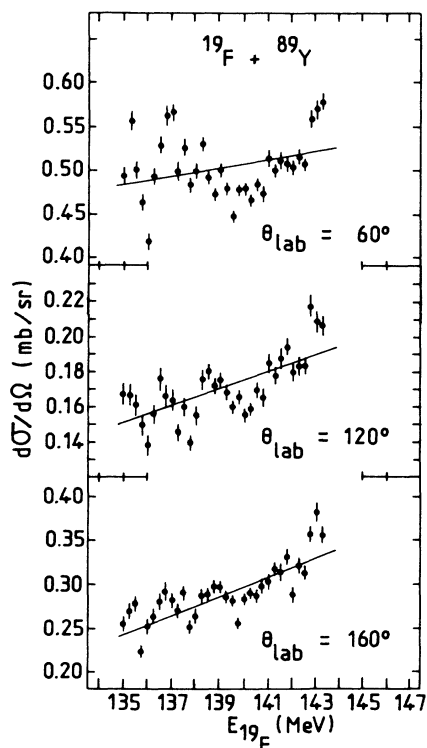


FIG. 5. Global excitation functions, at three different angles, for the $^{89}\text{Y}(^{19}\text{F},x)y$ reaction obtained by adding partial excitation functions of fragments $Z = 8, 10$, and 11 .

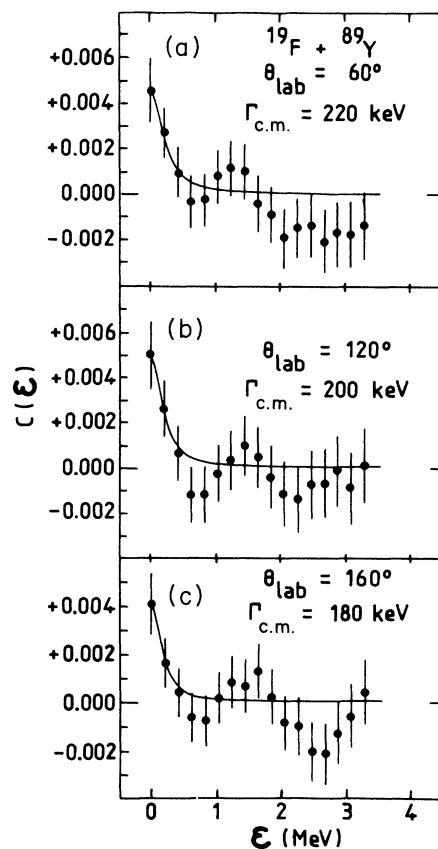


FIG. 6. Autocorrelation function of the excitation function of various ejectiles, detected at $\theta_{\text{lab}} = 160^\circ$, in the $^{89}\text{Y}(^{19}\text{F},x)y$ reaction.

TABLE I. Z cross-correlation coefficients for various Z ejectiles at $\theta_{\text{lab}} \simeq 60^\circ, 120^\circ,$ and 160° . The errors are due to the finite size of the data sample.

θ_{lab} (deg)	Z	5	6	7	8	10	11
60	5	1					
	6	0.80 ± 0.20	1				
	7	0.72 ± 0.14	0.80 ± 0.20	1			
	8	0.62 ± 0.12	0.70 ± 0.14	0.74 ± 0.15	1		
	10	0.63 ± 0.13	0.67 ± 0.13	0.65 ± 0.13	0.62 ± 0.12	1	
120	11	0.42 ± 0.08	0.51 ± 0.10	0.48 ± 0.10	0.54 ± 0.11	0.46 ± 0.09	1
	8				1		
	10				0.67 ± 0.13	1	
160	11				0.46 ± 0.09	0.53 ± 0.11	1
	7			1			
	8			0.75 ± 0.15	1		
	10			0.63 ± 0.12	0.70 ± 0.14	1	
	11			0.68 ± 0.14	0.71 ± 0.14	0.52 ± 0.10	1

Hence, it is clear that the fluctuations observed in the present work are not of statistical origin and are not imputable to a long lifetime nuclear process like compound nucleus deexcitation. We have, then, calculated the autocorrelation functions in energy.

B. Energy autocorrelation functions

The autocorrelation functions have been calculated to obtain a coherence width in energy. For each fragment of a given Z , and for each angle of measurement, we have calculated the autocorrelation function according to the relationship

$$C(\epsilon) = \left\langle \left[\frac{\sigma(E)}{\overline{\sigma(E)}} - 1 \right] \left[\frac{\sigma(E+\epsilon)}{\overline{\sigma(E+\epsilon)}} - 1 \right] \right\rangle, \quad (2)$$

where ϵ is the increment in energy and where the angular brackets stand for the arithmetical average. The average cross sections $\overline{\sigma(E)}$ and $\overline{\sigma(E+\epsilon)}$ correspond to the straight solid lines in Figs. 2–4. The functions $C(\epsilon)$, for the 160° data and for the $Z = 8, 10,$ and 11 summed cross sections, are presented, respectively, in Figs. 6 and 7. The

TABLE II. θ cross-correlation coefficients for various Z fragments. The errors are due to the finite size of the data sample.

θ_1 (deg)	θ_2 (deg)	Z	$C(\theta_1, \theta_2)$
60	120	8	0.68 ± 0.14
		10	0.40 ± 0.08
		11	0.53 ± 0.10
60	160	7	0.67 ± 0.13
		8	0.70 ± 0.14
		10	0.58 ± 0.11
		11	0.43 ± 0.09
120	160	8	0.54 ± 0.11
		10	0.64 ± 0.13
		11	0.29 ± 0.06

error bars have been calculated according to the formula in Table 3 of Ref. 9, and bias corrections (reported in our Table III) were also taken into account. In these figures the solid curves are the best fits to the points calculated by using the Ericson prediction for statistical fluctuations:

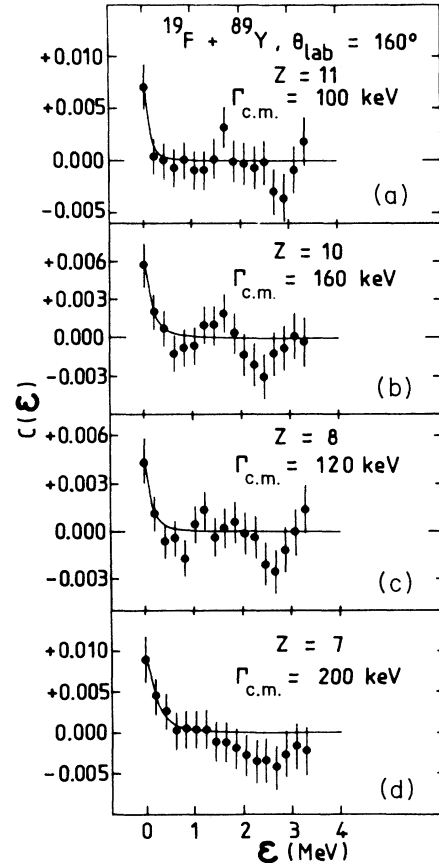


FIG. 7. Autocorrelation functions of the excitation functions given in Fig. 4 and corresponding to the sum of $Z = 8, 10,$ and 11 cross sections.

TABLE III. Comparison of the normalized variances $C(0)$ of the excitation functions of various Z fragments detected at different angles to the normalized variances due to statistical errors on the experimental data points, $C(0)=1/\bar{N}$, and to the Bias corrections.

θ_{lab} (deg)	Z	$C(0)$ ($\times 10^{-3}$)	$1/\bar{N}$ ($\times 10^{-3}$)	Bias ($\times 10^{-3}$)
60	7	5.2	0.6	0.5
	8	5.4	0.5	0.5
	10	5.3	1.1	0.5
	11	6.2	1.8	0.7
	$\sum Z=8+10+11$	4.6	0.3	0.5
120	8	5.2	1.9	0.6
	10	7.7	3.0	0.8
	11	10.9	3.6	1.2
	$\sum Z=8+10+11$	5.0	0.9	0.5
160	5	6.2	2.8	0.7
	6	4.3	0.8	0.4
	7	9.0	2.2	1.0
	8	4.5	1.7	0.5
	10	5.6	2.6	0.6
	11	7.0	3.3	0.8
	$\sum Z=8+10+11$	4.1	0.8	0.4

TABLE IV. Coherence widths Γ obtained by analyzing the energy autocorrelation functions of various Z fragments detected at $\theta_{\text{lab}}=60^\circ$, 120° , and 160° with the generalized Ericson model (Refs. 4 and 8) and deduced reaction lifetimes τ . The errors are due to the finite size of the data sample.

θ_{lab} (deg)	Z	$\Gamma_{\text{c.m.}}$ (keV)	τ ($\times 10^{-21}$ s)
60	7	160 \pm 40	4.1 \pm 0.8
	8	240 \pm 60	2.7 \pm 0.5
	10	120 \pm 30	5.5 \pm 0.9
	11	180 \pm 50	3.7 \pm 0.8
	$\sum Z=8+10+11$	220 \pm 60	3.0 \pm 0.7
120	8	180 \pm 50	3.7 \pm 0.8
	10	140 \pm 40	4.7 \pm 1.0
	11	140 \pm 40	4.7 \pm 1.0
	$\sum Z=8+10+11$	200 \pm 50	3.3 \pm 0.7
160	5	240 \pm 60	2.7 \pm 0.5
	6	240 \pm 60	2.7 \pm 0.5
	7	200 \pm 50	3.3 \pm 0.7
	8	120 \pm 30	5.5 \pm 0.9
	10	160 \pm 40	4.1 \pm 0.8
	11	100 \pm 30	6.6 \pm 1.5
	$\sum Z=8+10+11$	180 \pm 50	3.6 \pm 0.8

$$C(\epsilon) = (1/N_{\text{eff}})\Gamma^2 / (\Gamma^2 + \epsilon^2) . \quad (3)$$

In this relationship, N_{eff} is the number of effective outgoing channels and Γ is the coherence width, it represents the full width at half maximum of the $C(\epsilon)$ function. The maxima $C(0)$ of this function corresponds to the amplitude at the origin,⁸ i.e., at $\epsilon=0$. A relationship similar to (3) was recently derived by Brink and Dietrich⁴ for strongly damped deep inelastic collisions. In relationship (3), one sees that fluctuations can only be measurable when N_{eff} is not too large, which implies that these measurements are restricted to fairly light nuclear systems.

The autocorrelation functions $C(0)$ are reported in Table III, together with the quantities $1/\bar{N}$ where \bar{N} is the average counting rate for each measurement. These $1/\bar{N}$ ratios represent the autocorrelation functions corresponding only to statistical uncertainties on the data. Let us observe that at all three angles clear departures exist between $C(0)$ and $1/\bar{N}$. This confirms the fact that the fluctuations, analyzed here and shown in Figs. 2–5, are true fluctuations and do not result from insufficient statistics. Thus, coherence widths Γ and subsequent lifetimes τ can be extracted. They are reported in Table IV. The uncertainties are of the order of 25% and result from the finite size of the data samples. The lifetimes are all equal to some 10^{-21} s. They are reported in Fig. 8 as solid points, for the measurements performed at $\theta_{\text{lab}}=160^\circ$.

The lifetimes can also be extracted from another method, independent of that described above, namely the peak counting method.^{11,12} In this approach, the coher-

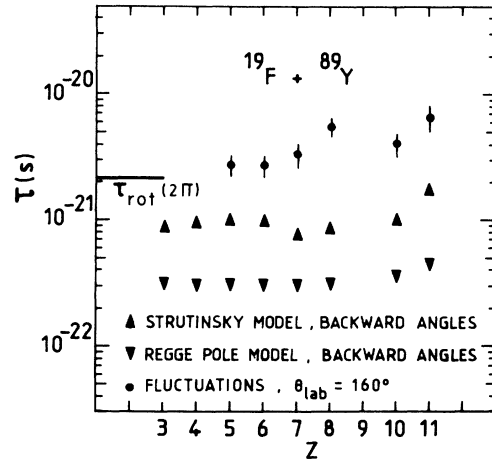


FIG. 8. Nuclear reaction lifetimes τ of various exit channels yielding fragments (identified by their Z) in the $^{89}\text{Y}(^{19}\text{F},x)\text{y}$ reaction studied at $\theta_{\text{lab}}=160^\circ$. The lifetimes have been deduced from different methods: an analysis of the autocorrelation function (solid points), an analysis of the angular distributions of the fragments in the backward hemisphere with the Strutinsky model (Refs. 6 and 7) (upright triangles) and an analysis of the same data with the Regge pole method (Refs. 5 and 6) (inverted triangles). The latter two analyses are presented in Refs. 1 and 2. The collision time corresponding to a complete nuclear rotation, $\tau_{\text{rot}}(2\pi)=2.1 \times 10^{-21}$ s, has been reported in the figure.

ence width Γ is derived from the formula

$$\Gamma = 0.5 \Delta E_{c.m.} / (b_{\infty} K_1), \quad (4)$$

where $\Delta E_{c.m.}$ is the total energy range in the center of mass over which the data are collected, $b_{\infty} = 0.707$ if N_{eff} is large, i.e., $C(0)$ very small, and K_1 is the number of maxima in the cross section over the energy range considered. In the present experiment, Γ is, on the average, equal to 510 keV and corresponds to a lifetime $\tau = 1.3 \times 10^{-21}$ s, slightly less than the values deduced from the autocorrelation function analysis.

V. DISCUSSION

The lifetime values deduced from the autocorrelation function analysis are all larger than 2×10^{-21} s. These values are quite comparable to those measured for other systems.^{3,13,14} Hence, an average value $\tau = 1.7 \times 10^{-21}$ s has been extracted for ^{12}C on ^{24}Mg .¹⁴ The values derived from the present autocorrelation analysis are moderately larger than those obtained in previous works^{1,2} from a data treatment based on the Strutinsky model^{6,7} and exceed by one order of magnitude the τ values deduced from a Regge pole analysis.^{5,6} All these τ values are also reported in Fig. 8, which summarizes the lifetime values obtained by three different and independent methods. For most of them, the deduced τ values are of the order of a complete rotation of the projectile around the target, i.e., $\tau_{rot}(2\pi) = 2.10 \times 10^{-21}$ s. These lifetimes are surprisingly long and may signify that the $^{19}\text{F} + ^{89}\text{Y}$ system exists as a

short-lived molecular configuration. Such quasimolecular resonances can produce correlated fluctuations in all the nearly equilibrated exit channels studied here. These resonances would play the role of doorway states in the entrance channel as similarly interpreted by other authors recently when measuring the $^{28}\text{Si} + ^{64}\text{Ni}$ system.¹⁴

The present results and interpretation are also consistent with the approach of Shivakumar *et al.*¹⁵ for the $^{28}\text{Si} + ^{14}\text{N}$ system. In this latter work, the authors observe orbiting configurations corresponding to a dinuclear system living long enough to permit the equilibration of charge and mass and to lead eventually to fusion. However, in this process a definite probability of reseparation in two nuclei exists. It may explain the present results.

VI. CONCLUSIONS

In this work we have measured the yields of the $5 \leq Z \leq 11$ ejectiles in the $^{19}\text{F} + ^{89}\text{Y}$ reaction around 140 MeV incident energy. Fluctuations have been observed and are shown not to be of statistical origin by Z and θ cross-correlation analyses. The autocorrelation functions have been calculated and the energy coherence widths derived for each fragment; the lifetimes further deduced are all larger than 2.7×10^{-21} s and exceed a full nuclear rotation lifetime. These results suggest that the outgoing fragments under investigation may result from quasimolecular configurations acting as doorway states in the entrance channel and/or from an orbiting dinuclear system which reseparates in two nuclei.

¹T. Suomijärvi, R. Lucas, M. C. Mermaz, J. P. Coffin, G. Guillaume, B. Heusch, F. Jundt, and F. Rami, *Z. Phys. A* **321**, 531 (1985).

²M. C. Mermaz, B. Berthier, R. Lucas, T. Suomijärvi, J. P. Coffin, G. Guillaume, B. Heusch, F. Jundt, and F. Rami, *Nucl. Phys. A* **456**, 186 (1986); T. Suomijärvi, thesis, Université Paris–XI, 1986 (unpublished).

³A. de Rosa, G. Inglima, V. Russo, M. Sandoli, G. Fortuna, G. Montagnoli, C. Signorini, A. M. Stefani, G. Cardella, G. Pappalardo, and F. Rizzo, *Phys. Lett.* **160B**, 239 (1985).

⁴D. M. Brink and K. Dietrich, *Z. Phys. A* **326**, 7 (1987).

⁵J. Barrette, P. Braun-Munzinger, C. K. Gelbke, H. E. Wegner, B. Zeidman, A. Gamp, H. L. Harney, and Th. Walcher, *Nucl. Phys. A* **279**, 125 (1977).

⁶C. K. Gelbke, C. Olmer, M. Buenerd, D. L. Hendrie, H. Mahoney, M. C. Mermaz, and D. K. Scott, *Phys. Rep.* **42**, 311 (1978).

⁷V. M. Strutinsky, *Phys. Lett.* **44B**, 245 (1973).

⁸T. E. O. Ericson, *Ann. Phys. (N.Y.)* **23**, 390 (1963); G. Pappalardo, *Phys. Lett.* **13**, 320 (1964).

⁹A. Richter, in *Nuclear Spectroscopy and Reactions*, edited by J. Cerny (Academic, New York, 1974), Vol. B, p. 343.

¹⁰D. M. Brink, R. O. Stephen, and N. W. Tanner, *Nucl. Phys.* **54**, 577 (1964).

¹¹D. M. Brink and R. O. Stephen, *Phys. Lett.* **5**, 77 (1963).

¹²A. Van der Woude, *Nucl. Phys.* **80**, 14 (1966).

¹³A. Glaesner, W. Dünneweber, W. Hering, D. Konnerth, R. Litzka, R. Sing, and W. Trombik, *Phys. Lett.* **169B**, 153 (1986).

¹⁴R. Bonetti and M. S. Hussein, *Phys. Rev. Lett.* **57**, 194 (1986).

¹⁵B. Shivakumar, D. Shapira, P. H. Nelson, M. Beckerman, B. A. Harmon, K. Teh, and S. Ayik, in *Proceedings of the Symposium on the Many Facets in Heavy-Ion Fusion Reactions*, Argonne (1986), pp. 407 and 605.